PLEKHA4 upregulation regulates KIRC cell proliferation through β-catenin signaling

YUYANG YUE[1], GUANGQI AN[2], SHUXIA CAO[3], XIANGDAN LI[4], LIPING DU[2], DONGYUAN XU[3], TOUFENG JIN[5] and LAN LIU[1]

[1]Department of Pathology, Yanbian University Hospital, Yanji, Jilin 133000, P.R. China; [2]Department of Ophthalmology, The First Affiliated Hospital of Zhengzhou University, Zhengzhou, Henan 450052, P.R. China; [3]Key Laboratory of Cellular Function and Pharmacology of Jilin Province, Yanbian University, Yanji, Jilin 133002, P.R. China; [4]Center of Morphological Experiment, Medical College of Yanbian University, Yanji, Jilin 133002, P.R. China; [5]Department of General Surgery, Yanbian University Hospital, Yanji, Jilin 133000, P.R. China

Received July 31, 2024; Accepted October 7, 2024

DOI: 10.3892/mmr.2024.13395

Abstract. In the present study, pleckstrin homology domain-containing family A member 4 (PLEKHA4) was identified as being upregulated in renal cell carcinoma, particularly within the kidney renal clear cell carcinoma (KIRC) subtype. The present study conducted bioinformatics analysis, Cell Counting Kit-8 and cell migration assays, flow cytometry, western blotting and *in vivo* experiments with the aim of uncovering the role of PLEKHA4 in β-catenin signaling in KIRC cells. Notably, PLEKHA4 upregulation was revealed to be associated with enhanced cell proliferation, indicating its potential role as an oncogene in KIRC. Mechanistically, knockdown of PLEKHA4 in KIRC cells led to decreased β-catenin signaling and cyclin D1 expression and the induction of cell cycle arrest at the G_1/S phase, suggesting that PLEKHA4 facilitated tumorigenesis through modulation of the Wnt/β-catenin pathway. PLEKHA4 knockdown also inhibited cell viability, migration and colony formation, further emphasizing its role in cancer progression. Notably, overexpression of PLEKHA4 activated Wnt/β-catenin signaling, reinforcing its role in promoting β-catenin nuclear translocation and signaling activity. The present findings suggested that PLEKHA4 could serve as a potential therapeutic target for KIRC; inhibiting PLEKHA4 or modulating Wnt/β-catenin signaling could provide new avenues for treatment strategies in KIRC.

Correspondence to: Professor Lan Liu, Department of Pathology, Yanbian University Hospital, 1327 Juzi Street, Yanji, Jilin 133000, P.R. China
E-mail: lliu@ybu.edu.cn

Professor Toufeng Jin, Department of General Surgery, Yanbian University Hospital, 1327 Juzi Street, Yanji, Jilin 133000, P.R. China
E-mail: tfjin@ybu.edu.cn

Key words: pleckstrin homology domain-containing family A member 4, kidney renal clear cell carcinoma, proliferation, β-catenin

Introduction

According to global clinical data, renal cell carcinoma (RCC) is the most lethal form of urogenital cancer, characterized by a mortality rate of 30-40% (1,2). Kidney renal clear cell carcinoma (KIRC) accounts for 70-80% of all RCC cases worldwide (3). Effective therapeutic targets and molecular drugs for KIRC are limited, rendering it difficult to treat. Notably, the incidence of KIRC has been steadily increasing in recent years. From 2000 to 2016, countries such as Japan, Italy and the USA experienced an increase in age-standardized rate of RCC, rising from 5.3, 12 and 10.7 per 100,000 to 7.8, 13.7 and 13.3 per 100,000, respectively (1,4). And KIRC displays resistance to radiotherapy, chemotherapy and immunotherapy, underscoring surgery as the primary treatment modality (5). Among patients with KIRC, 60% exhibit a survival duration of 1-2 years post-diagnosis, with 30% manifesting distant metastasis at the time of diagnosis globally (2). Therefore, the identification of effective therapeutic targets is key for early diagnosis and intervention in KIRC.

Pleckstrin homology domain-containing family A member 4 (PLEKHA4) is as a key molecular player in cancer biology, particularly in glioma (6,7). It serves multiple roles in cancer progression, operating through diverse mechanisms. In glioblastoma, PLEKHA4 is involved in the regulation of apoptotic regulators, exerting an inhibitory effect on apoptosis. Moreover, PLEKHA4 triggers dishevelled accumulation and promotes the upregulation of Wnt signaling in cultured mammalian cells, including human HeLa, 293T and 293, and mouse C57MG and MV7 Rat2a cells (8).

Dysregulated Wnt signaling has been associated with a spectrum of diseases, encompassing embryonic malformations, degenerative disorders and cancer. Perturbations in β-catenin function can stem from diverse origins, including extracellular cues, cytoplasmic components and nuclear factors (9). Aberrations in β-catenin activities are linked to the development of various human degenerative disorders and numerous types of cancer, including those affecting the breast, colon and kidney (10-12). Consequently, the involvement of

β-catenin in these mechanisms has spurred investigation, including in the context of KIRC (4,13). In oncogenesis, aberrant Wnt/β-catenin signaling amplifies the activation of its target genes, such as cyclin D1, which serve a crucial role in the pathway (14). Despite the high expression of PLEKHA4 observed in various types of cancer, such as glioma and melanoma (7,8), the precise mechanisms by which it influences KIRC progression remain inadequately elucidated. The present study investigated the role of PLEKHA4 in KIRC to improve understanding of the molecular mechanisms underlying KIRC and to facilitate the development of novel therapeutic approaches.

Materials and methods

Bioinformatics analysis. Pan-cancer analysis and gene set variation analysis (GSVA) were performed using Gene Set Cancer Analysis (GSCA; https://guolab.wchscu.cn/GSCA/#/). GSVA was performed to estimate the integrated level of gene set expression for each The Cancer Genome Atlas (TCGA) sample. The gene expression profiles GSE15641 (15) and GSE40435 (16), which were obtained with the GPL96 platform, were retrieved from Gene Expression Omnibus (GEO; https://www.ncbi.nlm.nih.gov/geo/). The GSE15641 profile encompassed data from 49 RCC tumors, 20 non-RCC renal tumors and 23 normal kidney samples. The GSE40435 profile included information from 101 pairs of KIRC and adjacent non-tumor renal samples. The data from the GEO database were processed using GEOquery (2.64.2) (https://bioconductor.org/packages/release/bioc/html/GEOquery.html) and subsequent normalization was performed using the normalizeBetweenArrays function from the limma package (3.52.2) (https://www.bioconductor.org/packages/release/bioc/html/limma.html). The outcomes were visualized using ggplot2 (3.3.6) (https://cran.r-project.org/src/contrib/Archive/ggplot2/) and ComplexHeatmap (2.13.1) (https://github.com/jokergoo/ComplexHeatmap). Calibration, standardization and log2 transformation were applied to all gene expression data. Kyoto Encyclopedia of Genes and Genomes (KEGG) and Gene Ontology (GO) analyses were performed using clusterProfiler [4.4.4] (https://bioconductor.org/packages/release/bioc/html/clusterProfiler.html) and GOplot [1.0.2] (https://cran.r-project.org/web/packages/GOplot/index.html). The expression patterns of PLEKHA4 across pathological and histological grades were assessed using R (version 4.2.1) (https://www.r-project.org/) and visualized utilizing ggplot2 (3.3.6). RNA sequencing data were obtained from TCGA-KIRC project through the STAR pipeline of TCGA database (https://www.cancer.gov/ccg/research/genome-sequencing/tcga), with the data extracted in TPM format. Gene Mania (https://genemania.org/) was also used to explore the interaction between genes.

Cell culture. Human KIRC cell lines 769-P, 786-O and CAKI1 were procured from the National Collection of Authenticated Cell Cultures. According to the depmap portal (The Cancer Dependency Map Project at Broad Institute; https://depmap.org/portal/), PLEKHA4 is highly expressed in 769-P and 786-O cell lines, and is expressed at lower levels in CAKI1 cell lines. The 769-P and 786-O cell lines were used for knockdown assays, and the CAKI1 cell line for overexpression assays.

Briefly, 769-P and 786-O cells were maintained in RPMI-1640 medium (Gibco; Thermo Fisher Scientific, Inc.) supplemented with 10% FBS and 1% penicillin-streptomycin, and CAKI1 cells were cultured in DMEM (Gibco; Thermo Fisher Scientific, Inc.) supplemented with 10% FBS (Biological Industries; Sartorius AG) and 1% penicillin-streptomycin (Biological Industries; Sartorius AG). Cell cultures were maintained in a 37˚C incubator with 5% CO_2. For drug treatment, lithium chloride (LiCl, Selleck Chemicals) at a concentration of 5 mM was added to the medium and incubated for 12 h in a 37˚C incubator with 5% CO_2 to activate the Wnt/β-catenin signaling pathway.

Cell transduction and transfection. 769-P and 786-O cells were transduced with short hairpin RNA (shRNA) lentiviruses targeting PLEKHA4. The two shRNAs used were Sh1 [K7453 LV3(H1/GFP&Puro)-PLEKHA4-Homo-2851; target sequence: 5'-GCGAGTCACTCTGCTACAATC-3'] and Sh2 [K7451 LV3(H1/GFP&Puro)-shPLEKHA4#2; target sequence: 5'-AGCTACAATATTAGACCAGA-3'], along with a negative control (NC) lentivirus (LV3-shNC; target sequence: 5'-GTTCTCCGAACGTGTCACGT-3'). These lentiviruses were produced by Shanghai GenePharma Co., Ltd.

The 3rd generation system was used for lentiviral transduction. Briefly, 293T cells (National Collection of Authenticated Cell Cultures) were used to produce the viruses using the recombinant shuttle and packaging plasmids pGag/Pol, pRev and pVSV-G. The concentration and purity of the plasmids were measured using UV absorption, ensuring that the A260/A280 ratio of the extracted plasmid DNA was between 1.8 and 2.0. The recombinant plasmid and packaging plasmids were mixed in a ratio of 8:4:4:4 μg (sh1,sh2 or NC:pGag/Pol:pRev:pVSV-G), and were added to the 293T cells and incubated in a 37˚C incubator containing 5% CO_2 for 4-6 h. After removing the mixture, culture medium was added and incubation was continued for 72 h in a 37˚C incubator containing 5% CO_2. The supernatant was then collected from the dishes and cell debris was removed by passing it through a 0.45-μm filter. Viral particles were concentrated by ultracentrifugation at 70,000 x g for 2 h at 20˚C using conical tubes and a swinging bucket rotor. The pellets were then resuspended in 100 μl 1X HBSS (cat. no. 14025-092; Invitrogen; Thermo Fisher Scientific, Inc.). An additional 100 μl 1X HBSS was added to the tubes, bringing the final volume to 200 μl, which was transferred to a screw-cap microfuge tube, wrapped in parafilm and vortex at low speed for 15-30 min. After resuspension, the tube was briefly spun for 10 sec, the supernatant was transferred to a fresh tube and 20-μl aliquots were generated. The aliquots were stored at -20˚C for up to 1 month or at -80˚C for longer, avoiding more than three freeze-thaw cycles. Lentiviral infection was carried out immediately after the virus preparation. The virus titers were as follows; sh1 (LV3-PLEKHA4-Homo-2851), $7x10^8$ TU/ml, sh2 (shPLEKHA4#2), $7x10^8$ TU/ml and shNC (LV3-shNC), $9x10^8$ TU/ml. The multiplicity of infection (MOI) values of sh1, sh2 or shNC in 769-P cells were 5, 10 and 10; and the MOI values of sh1, sh2 or shNC in 786-O cells was 10, 20 and 15. After 72 h of transfection and virus collection, the lentiviruses were added to the cells and were incubated for 24 h for gene transduction. Polybrene (2 μg/ml) was mixed with the virus

prior to adding it to the cells to enhance infection efficiency. Following transduction, cells were subjected to selection with 1 μg/ml puromycin for 7 days; the same concentration (1 μg/ml) was used for maintenance. The infection efficacy was assessed through western blot analysis. Western blotting and other experiments were performed immediately after the 7-day puromycin selection.

To induce PLEKHA4 overexpression in CAKI1 cells, pIRES2-EGFP-PLEKHA4 or control vector (pIRES2-EGFP-empty) plasmids were obtained from Shanghai GenePharma Co., Ltd. Plasmids were transfected into cells at 70% confluence using EndoFectin MAX (GeneCopoeia, Inc.). For transfection in a 6-well plate, 2.5 μg plasmids and 5-12.5 μl EndoFectin MAX were diluted with serum-free DMEM, each in 125 μl and were left for 5 min. Subsequently, they were mixed gently and the mixture was left for 5-20 minto form the DNA-EndoFectin complex, which was added to cells in the wells of a 6-well plate. The cells were incubated in a CO_2 incubator at 37˚C. Gene expression could be detected 48 h after transfection.

Cell proliferation assay. The 769-P and 786-O cells were plated in 96-well plates at a density of 3,000 cells/well and cultured for 0, 24, 48, 72 and 96 h. Subsequently, cells were treated with 10 μl Cell Counting Kit-8 (Shanghai Yeasen Biotechnology Co., Ltd.) solution and incubated for 1 h at 37˚C. The absorbance values were measured at 450 nm. Each experiment was replicated ≥3 times.

Colony formation assay. The transduced 769-P and 786-O cells were seeded in 6-well plates at a concentration of $5x10^3$ cells/well and incubated for 7 days. At room temperature, cells were washed twice with PBS, fixed with 4% paraformaldehyde for 15 min and subsequently stained with Giemsa (both Beijing Solarbio Science & Technology Co., Ltd.) for 20 min, before being washed twice again with PBS. A colony was defined as containing a minimum of 50 cells and colonies were quantified using ImageJ, bundled with 64-bit Java 8 (https://imagej.net/ij/index.html; National Institutes of Health).

Wound healing assay. The 769-P and 786-O cells were seeded in 6-well plates at a density of $1x10^6$ cells/well and grown to 90% confluence. Subsequently, the cells were incubated overnight in serum-free medium. The cell monolayers were then mechanically wounded using a 10-μl pipette tip. Images of the wounds were captured at 0 and 24 h using a Nikon Eclipse Ti-S/L100 Inverted Phase Contrast Fluorescent Microscope (Nikon Corporation) with a 10X objective. The wound was measured using ImageJ, bundled with 64-bit Java 8 and statistical analysis was performed using SPSS 29 (IBM Corp.). Each experiment was conducted a minimum of three times.

Flow cytometric analysis of cell cycle progression. After trypsinizing the cells without EDTA, cells were centrifuged at 300 x g for 5 min at 4˚C. Cells were then washed twice with pre-cooled PBS and resuspended in 100 μl 1X Binding Buffer (Shanghai Yeasen Biotechnology Co., Ltd.). The cells were then incubated with RNase A and PI Staining Solution (Shanghai Yeasen Biotechnology Co., Ltd.) in the dark at room temperature for 10-15 min. Finally, 400 μl 1X Binding Buffer (Shanghai Yeasen Biotechnology Co., Ltd.) was added on ice. The samples were analyzed using a flow cytometer CytoFLEX SRT (Beckman Coulter, Inc.) within 1 h. FlowJo V8 (FlowJo, LLC) was used for analysis.

Western blotting. Briefly, 769-P and 786-O cells, and genetically transduced 769-P, 786-O and CAKI1 cells were seeded in 6-well plates at a density of $1x10^6$ cells/well and cultured in RPMI-1640 or DMEM containing 10% FBS until they reached ~90% confluence. Protein lysate was extracted using RIPA buffer (Beijing Solarbio Science & Technology Co., Ltd.). Nuclear protein extraction was performed using the Nuclear and Cytoplasmic Extraction kit (Invitrogen; Thermo Fisher Scientific, Inc.) according to the manufacturer's instructions. Protein concentration was determined using the BCA Protein Assay Kit (Beyotime Institute of Biotechnology). Proteins (30 μg/lane) were separated by SDS-PAGE on 8-10% gels, transferred onto PVDF membranes and blocked with 5% non-fat dry milk (MilliporeSigma) at room temperature for 1 h, then incubated with primary antibodies overnight. The following primary antibodies were used: PLEKHA4 (cat. no. NBP1-56679; Novus Biologicals; Bio-Techne), β-actin (cat. no. GB12001-100; Wuhan Servicebio Technology Co., Ltd.), β-catenin (cat. no. AF6266; Affinity Biosciences), phosphorylated (p-)GSK3β (cat. no. sc-373800; Santa Cruz Biotechnology, Inc.), GSK3β (cat. no. sc-377213; Santa Cruz Biotechnology, Inc.), cyclin D1 (cat. no. AF0931; Affinity Biosciences) and Lamin B1 (cat. no. sc-374015; Santa Cruz Biotechnology, Inc.). The primary antibodies were diluted at 1:1,000 in Primary Antibody Dilution Buffer (Beyotime Institute of Biotechnology) and were incubated with the membranes at 4˚C overnight. Subsequently, the blots were probed with HRP-conjugated anti-rabbit and anti-mouse secondary antibodies (cat. nos. RGAR001 and RGAM001; Proteintech Group, Inc.). The secondary antibodies were diluted at 1:5,000 in Tris-buffered saline-0.1% Tween 20 solution and were incubated with the membranes at room temperature for 2 h. ECL Western Blotting Substrate (Beijing Solarbio Science & Technology Co., Ltd.) was used to visualize the blots using the Shenhua Science Technology Co., Ltd. system. The grayscale values of proteins were measured using ImageJ, bundled with 64-bit Java 8. Each experiment was conducted ≥3 times.

Animal studies. The animal experiments were approved by the Laboratory Animal Ethics Committee Yanbian University (approval no. YD20230911020; Yanji, China). Briefly, 4-week-old male nude mice (average weight, 14 g), were procured from the Experimental Animal Center of Yanbian University and were randomly divided into two groups (n=5/group): The shNC group and the shPLEKHA4 group. Nude mice were housed in a specific pathogen-free environment with a temperature of 25˚C and humidity of 30%. The mice were exposed to a 12-h light/dark cycle and were fed adult mouse feed sterilized with cobalt-60. The water provided was sterilized by autoclaving. Access to food and water was free. The mice were subcutaneously injected with a 200-μl solution containing $5x10^6$ 769-P cells transduced with sh-NC or sh-PLEKHA4 in the right flank. Tumor size was monitored every 2 days. After 15 days, the animals were

humanely euthanized for tissue collection. The following humane endpoints were applied: Tumor weight must not exceed 10% of the normal body weight of the mice, and the diameter of the tumor in any direction on the body surface of adult mice must not exceed 20 mm. All mice were euthanized by cervical dislocation following anesthesia with intravenous injection of sodium pentobarbital at a dose of 70 mg/kg body weight. Death was confirmed by the absence of respiration and heartbeat for >5 min.

Hematoxylin and eosin (H&E) staining and immunohistochemistry (IHC). The subcutaneous tumors were fixed in 10% formalin at room temperature for 24 h, dehydrated in graded ethanol and embedded in paraffin. The paraffin-embedded tumors were sectioned into 4-μm slices. The slices were then oven-baked at 56˚C overnight and stained using the H&E Stain kit (Beijing Solarbio Science & Technology Co., Ltd.), according to the manufacturer's protocol.

For IHC, the slides were placed in 10 mM sodium citrate buffer (pH 6.0) and boiled, then simmered for 10 min, for antigen retrieval. Subsequently, the slides were cooled on the bench for 30 min. To remove endogenous peroxidase activity, slides were incubated with 3% hydrogen peroxide aqueous solution, limiting the exposure time to ~10 min at room temperature. Furthermore, blocking was performed using TBS- 0.1% Tween with 5% normal goat serum (Cell Signaling Technology, Inc.). The sections were then incubated overnight at 4˚C with primary antibodies against PLEKHA4 (1:200 dilution; cat. no. NBP1-56679; Novus Biologicals; Bio-Techne). The next day, a biotinylated Goat Anti-Rabbit IgG H&L (Biotin) secondary antibody (1:100; cat. no. ab207995; Abcam) was added, and the slides were incubated at room temperature for 30 min. Then streptavidin-horseradish peroxidase (cat. no. SA10001; Invitrogen; Thermo Fisher Scientific, Inc.) was then used to incubate the slides at room temperature for 30 min and 200 μl DAB was added to each slice as the chromogen. Hematoxylin was used to counterstain the slices at room temperature for 1 min. Finally, images of the slides were captured using a Nikon Eclipse Ti-S/L100 Inverted Phase Contrast Fluorescent Microscope with a 10X objective.

Statistical analysis. Statistical analysis was conducted using unpaired Student's t-test to compare the differences between two groups, while one-way ANOVA with Tukey's post hoc analysis was performed for comparisons among multiple groups. Data analysis was performed using SPSS 26.0 (IBM Corp.). The data are presented as the mean ± SD. Each experiment was replicated ≥3 times. $P<0.05$ was considered to indicate a statistically significant difference.

Results

PLEKHA4 is upregulated in KIRC and is associated with β-catenin signaling. GSCA was used to perform a comprehensive pan-cancer analysis to investigate the expression patterns of PLEKHA4 in human cancer tissues. PLEKHA4 was upregulated in numerous types of cancer, including KIRC (Figs. 1A and 2A). Based on data from GEO datasets, tumor tissues exhibited distinctive gene expression profiles compared with normal tissue (a mix of healthy control tissues and normal tissues adjacent to the cancer tissues) (Fig. 1B and E). The heatmaps illustrate the elevated expression of PLEKHA4 in renal tumors and KIRC tissue (Fig. 1C and F). Furthermore, GO and KEGG analyses revealed the upregulation of genes enriched in the 'Wnt signaling pathway' in both renal tumors and KIRC tissue (Fig. 1D and G). The results of both GO and KEGG analyses are presented as combined outcomes. To elucidate PLEKHA4 expression in KIRC, GSVA was used; there was a higher GSVA score in KIRC compared with in normal kidney tissue (Fig. 2B). GSVA scores represent the degree to which the genes in the gene set are coordinately up- or downregulated within that sample. In addition, GSVA scores were evaluated across various subtypes and stages of KIRC (Fig. 2C and D). PLEKHA4 expression in different pathological and histological grades of KIRC demonstrated significantly elevated levels in comparison with normal kidney tissue (Fig. 2E-I). Across various pathological stages, PLEKHA4 expression was consistently higher in cancerous tissues compared with in normal tissue (Fig. 2E). Specifically, when splitting patients according to pathological T stage, both T2&T1 and T3&T4 stage tissues exhibited elevated PLEKHA4 levels compared with in normal tissues from healthy individuals (Fig. 2F). Similarly, when splitting patients according to pathological N stage, tissues from patients with both N0 and N1 cancer showed increased PLEKHA4 expression (Fig. 2G) compared with in normal tissues from healthy individuals. Regarding pathological M stage, tissues from patients with both M0 and M1 cancer demonstrated higher PLEKHA4 levels (Fig. 2H) compared with in normal tissues from healthy individuals. Additionally, all stages (I, II, III, IV) and histologic grades (G1, G2, G3, G4) of KIRC exhibited elevated PLEKHA4 expression compared with that in normal tissues from healthy people (Fig. 2I).

PLEKHA4 knockdown inhibits KIRC cell proliferation. In order to assess PLEKHA4 expression in KIRC and normal tissues, the Human Protein Atlas (https://www.proteinatlas.org/) was used, which aims to map all human proteins in cells, tissues and organs using technologies such as antibody-based imaging, proteomics, transcriptomics and systems biology. High expression levels of PLEKHA4 were observed in KIRC tissue (Fig. 3A), and its levels in were also examined KIRC cells (Fig. 3B); 786-O and 769-P cells had higher PLEKHA4 levels than CAKI1 cells. Subsequently, PLEKHA4 knockdown experiments were conducted in 769-P and 786-O cells. The virus infection efficiencies of K7453 in 769-P and 786-O cells were 68 and 41%, respectively, while those of K7451 were 73 and 57%, respectively. For LV3-shNC, the transfection efficiencies in 769-P and 786-O cells were 63 and 54%, respectively. Protein levels in normal KIRC and PLEKHA4 knockdown cells were evaluated using western blot analysis. The results demonstrated a significant decrease in PLEKHA4 protein expression in 769-P and 786-O cells following knockdown (Fig. 3C). Proliferation, colony formation and migration assays indicated that PLEKHA4 knockdown inhibited cell proliferation (Fig. 3D), colony formation (Fig. 3E) and migration (Fig. 3F).

Knockdown of PLEKHA4 inhibits KIRC cell malignancy. Flow cytometric analysis was conducted to examine the cell cycle following PLEKHA4 knockdown. The results revealed

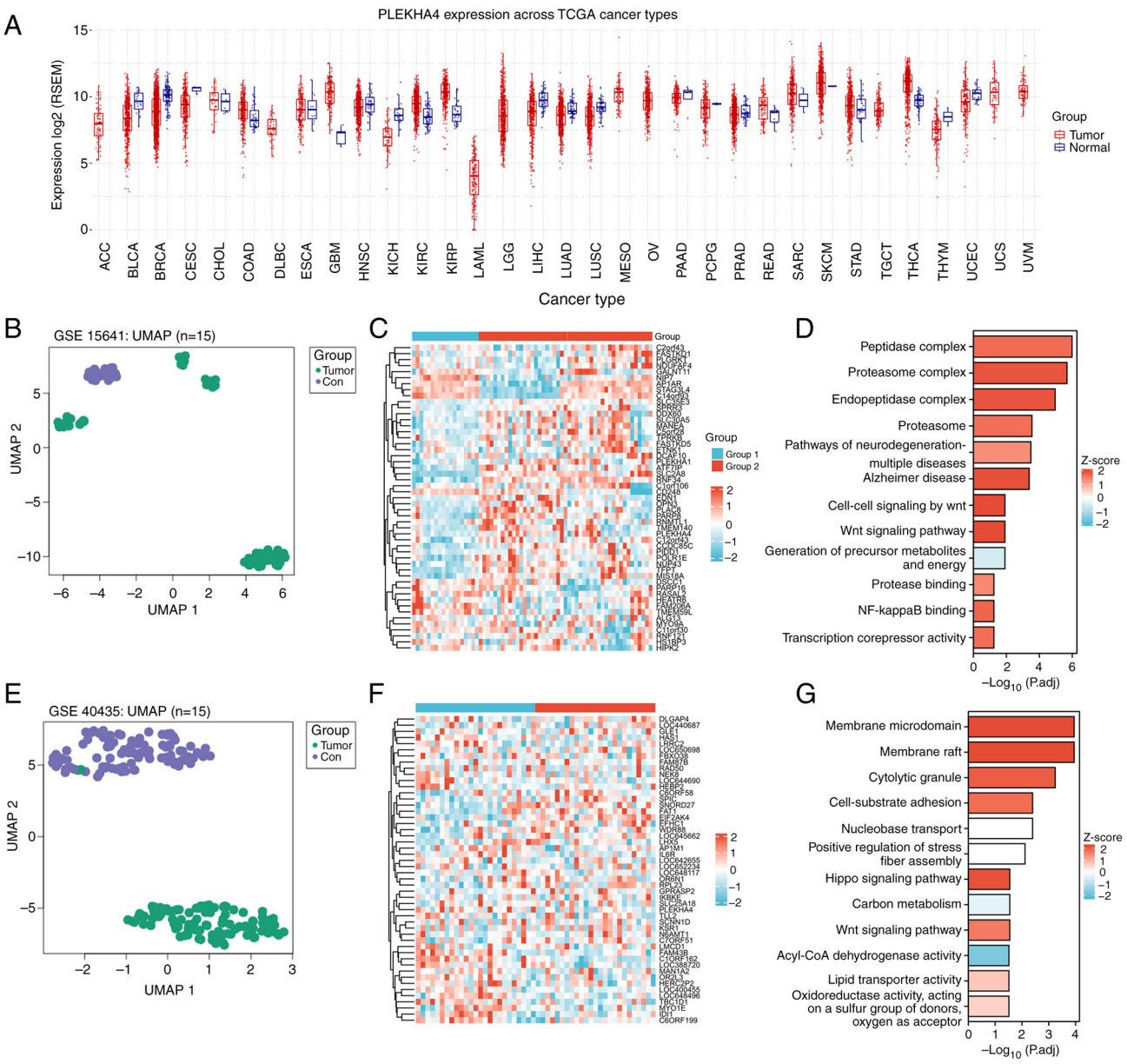

Figure 1. PLEKHA4 mRNA expression and analysis of two datasets reveal gene expression characteristics of KIRC. (A) PLEKHA4 mRNA expression in cancer was analyzed by Gene Set Cancer Analysis database. (B) UMAP of GSE15641 showed that renal tumors had a distinct proteomic profile compared with normal tissues. (C) Heatmap of gene expression profiles from GSE15641. (D) KEGG analysis of gene expression profiles from GSE15641. (E) UMAP of GSE40435 showed that KIRC tumors had a distinct proteomic profile compared with normal tissues. (F) Heatmap of gene expression profiles from GSE40435. (G) KEGG analysis of gene expression profiles from GSE40435. PLEKHA4, pleckstrin homology domain-containing family A member 4; KEGG, Kyoto Encyclopedia of Genes and Genomes; KIRC, kidney renal clear cell carcinoma; Con, control; TCGA, The Cancer Genome Atlas; UMAP, Uniform Manifold Approximation and Projection.

G_1/S phase arrest in the two KIRC cell lines (Fig. 4A). Subsequently, a subcutaneous tumor growth model was established to investigate the impact of PLEKHA4 on tumor growth. The knockdown of PLEKHA4 attenuated tumor growth (Fig. 4B-D). Tumor samples were collected and subjected to H&E staining and IHC to assess PLEKHA4 expression *in vivo*. Cells within the SHPLEKHA4 group exhibited lighter staining and were a smaller size with increased heterogeneity compared with those in the shNC group (Fig. 4E).

PLEKHA4 regulates Wnt/β-catenin signaling in KIRC cells. Given the observed upregulation of Wnt signaling in KIRC, Gene Mania was used to explore the interaction between PLEKHA4 and proteins associated with β-catenin (Fig. 5A). The results indicated that PLEKHA4 may have interactions with GSK3β and β-catenin. Following PLEKHA4 knockdown in 769-P and 786-O cells, western blotting revealed a reduction in the expression levels of p-GSK3β, β-catenin and cyclin D1 (Fig. 5B). The translocation of β-catenin into the nucleus is crucial for initiating gene transcription and driving tumorigenesis (14). PLEKHA4 knockdown resulted in decreased β-catenin levels in the nuclear fraction compared with in shNC cells, while cytosolic β-catenin levels were increased (Fig. 5C). In 786-O and 769-P cells, cytoplasmic β-catenin expression was significantly lower than nuclear expression in the shNC group. Conversely,

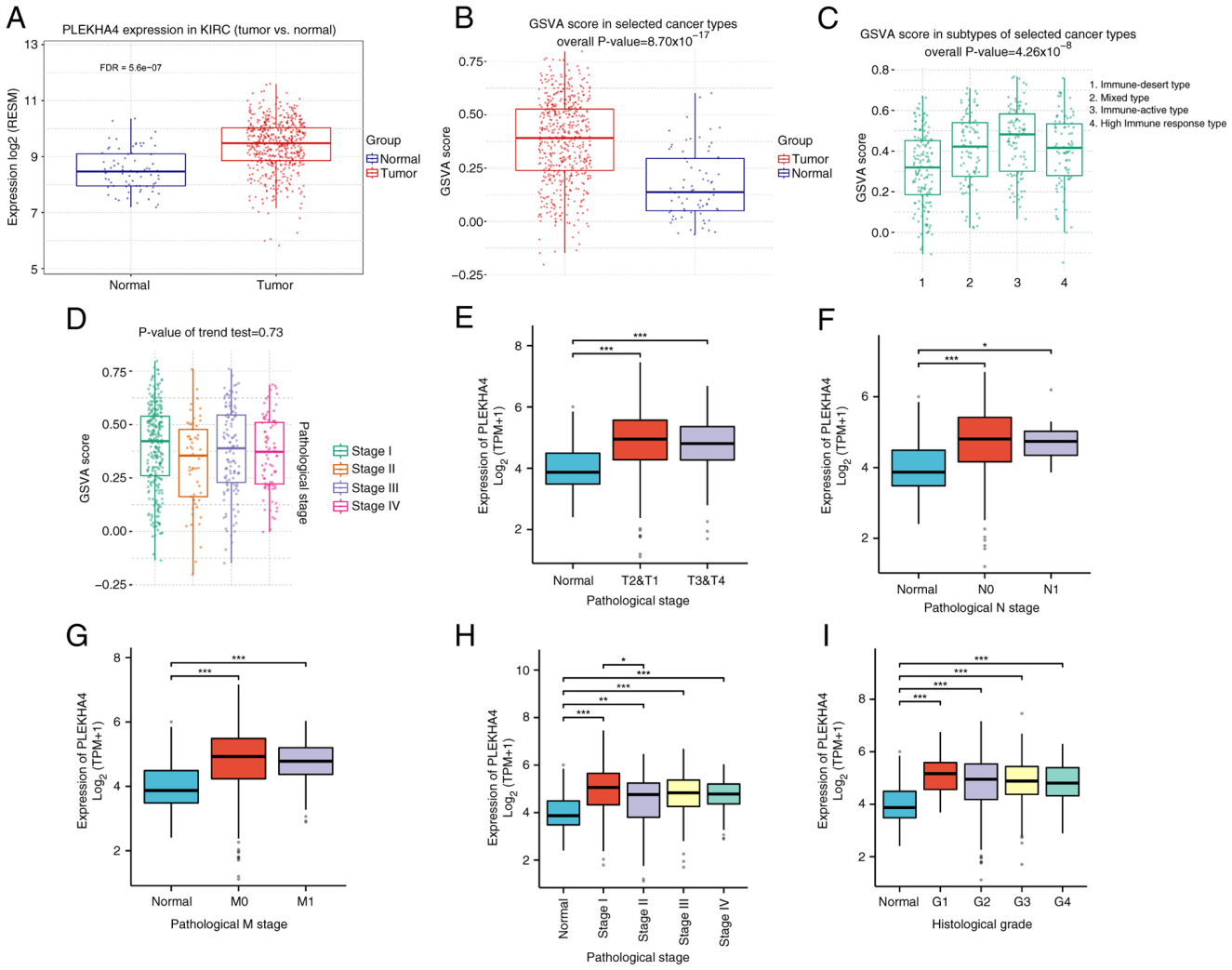

Figure 2. Analysis of PLEKHA4 expression in KIRC tissues and its association with different subtypes and stages. (A) Single gene level analysis in GSCA showed that PLEKHA4 expression is higher in KIRC tissues than in normal tissues. (B) KIRC tissue has a higher GSVA score than normal tissue, as analyzed by GSCA. GSVA scores in different KIRC (C) subtypes and (D) stages were analyzed by GSCA. PLEKHA4 expression in all (E) T, (F) N and (G) M stages of KIRC was higher than in normal tissue. PLEKHA4 expression in different (H) pathological stages and (I) grades of KIRC was higher compared with in normal tissue. *P<0.05, **P<0.01, ***P<0.001. GCSA, Gene Set Cancer Analysis; PLEKHA4, pleckstrin homology domain-containing family A member 4; KIRC, kidney renal clear cell carcinoma; GSVA, gene set variation analysis; FDR, false discovery rate.

in sh1- and sh2-transfected cells, cytoplasmic β-catenin expression was significantly higher than nuclear expression. This indicates that PLEKHA4 may facilitate the nuclear translocation of β-catenin, since knockdown of PLEKHA4 reduced the nuclear translocation of β-catenin. Lamin B1 was used as a marker to compare β-catenin expression levels in the nucleus with those in the cytoplasm (Fig. 5C), suggesting that PLEKHA4 promoted the nuclear translocation of β-catenin. To investigate the impact of PLEKHA4 on the Wnt/β-catenin pathway, KIRC cells were also treated with the Wnt signaling activator LiCl following PLEKHA4 knockdown. Western blotting demonstrated that LiCl reversed alterations induced by PLEKHA4 knockdown (Fig. 5D). Furthermore, overexpression was conducted to examine the role of PLEKHA4 on CAKI1 cells. PLEKHA4 overexpression led to an upregulation of proteins associated with Wnt/β-catenin signaling (Fig. 5E). These findings indicated that PLEKHA4 may serve a regulatory role in Wnt/β-catenin signaling in KIRC cells.

Discussion

Kidney cancer accounts for 2-3% of all cancer cases worldwide and is considered one of the most common types of urological malignancy, with >330,000 new cases reported each year (4,7). Renal cancer is a complex disease comprising different subtypes, with KIRC being the most predominant form. This subtype is associated with a widespread and deadly condition, with 431,288 new cases and 179,368 deaths reported globally in 2020 (6), underscoring the importance of improving the understanding of its biological attributes (7). A key challenge is a lack of clear understanding regarding the underlying mechanisms of KIRC (4). PLEKHA4, also known as PEPP1, encodes a protein featuring a pleckstrin homology domain positioned near the N-terminus and harbors a putative phosphatidylinositol 3,4,5-trisphosphate binding motif (6). PLEKHA4 has been shown to be upregulated in glioblastoma and inhibits apoptosis by modulating apoptotic regulators. The present study focused on the role of PLEKHA4 in KIRC,

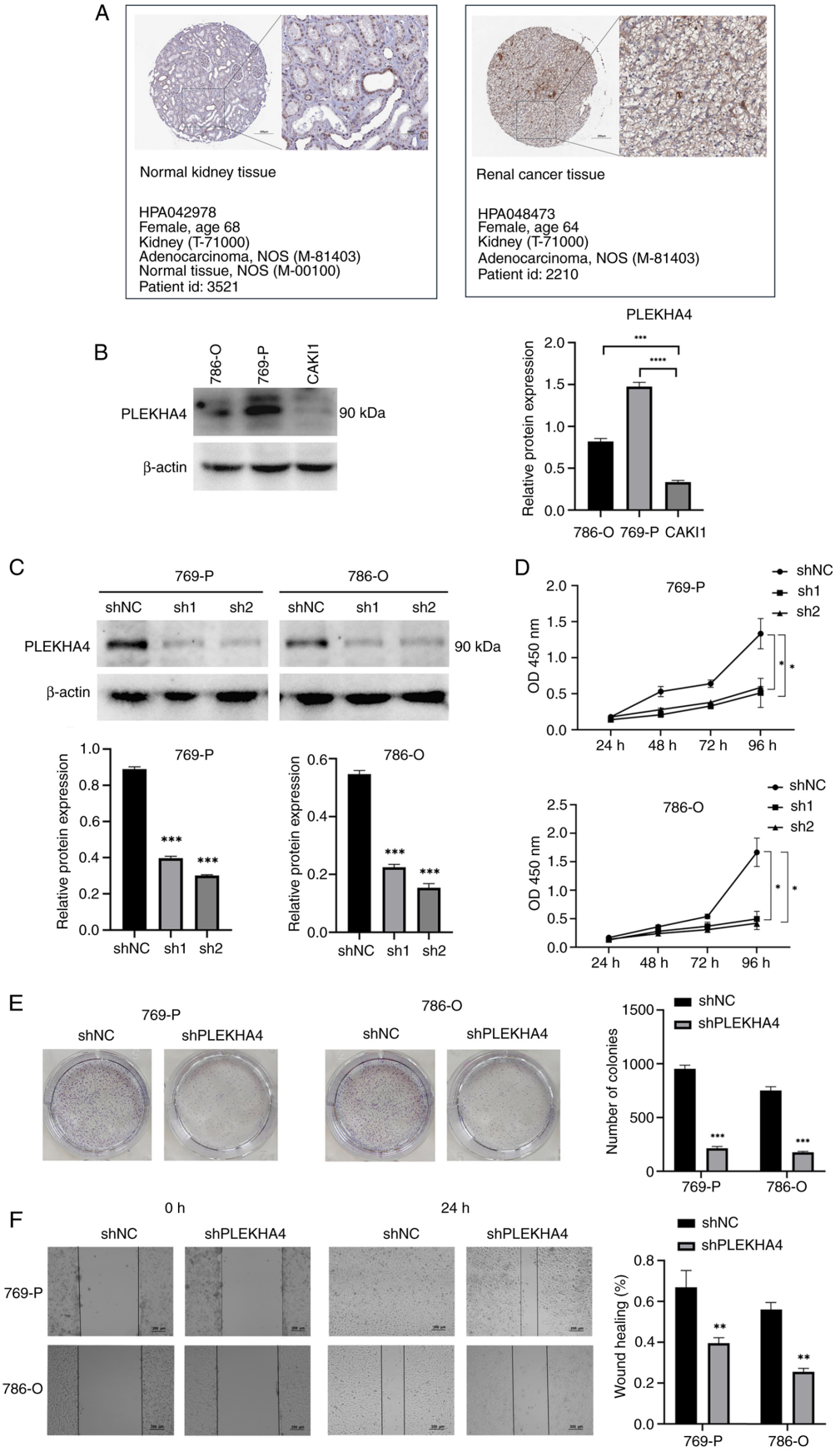

Figure 3. Effects of PLEKHA4 knockdown on kidney renal clear cell carcinoma cell proliferation, colony formation and migration. (A) Immunohistochemical staining with PLEKHA4 antibody on pathological slides from The Human Protein Atlas. (B) Western blotting to show the expression of PLEKHA4 in 786-O, 769-P and CAKI1 cells. (C) Western blotting to demonstrate the knockdown of PLEKHA4 in 769-P and 786-O kidney renal clear cell carcinoma cell lines. (D) Proliferation of 769-P and 786-O cells with PLEKHA4 knockdown was assessed using Cell Counting Kit-8 assay. Knockdown of PLEKHA4 expression inhibited (E) colony-forming and (F) migratory ability of 769-P and 786-O cells. *P<0.05, **P<0.01, ***P<0.001, ****P<0.0001 vs. shNC or as indicated. PLEKHA4, pleckstrin homology domain-containing family A member 4; sh, short hairpin; NC, negative control.

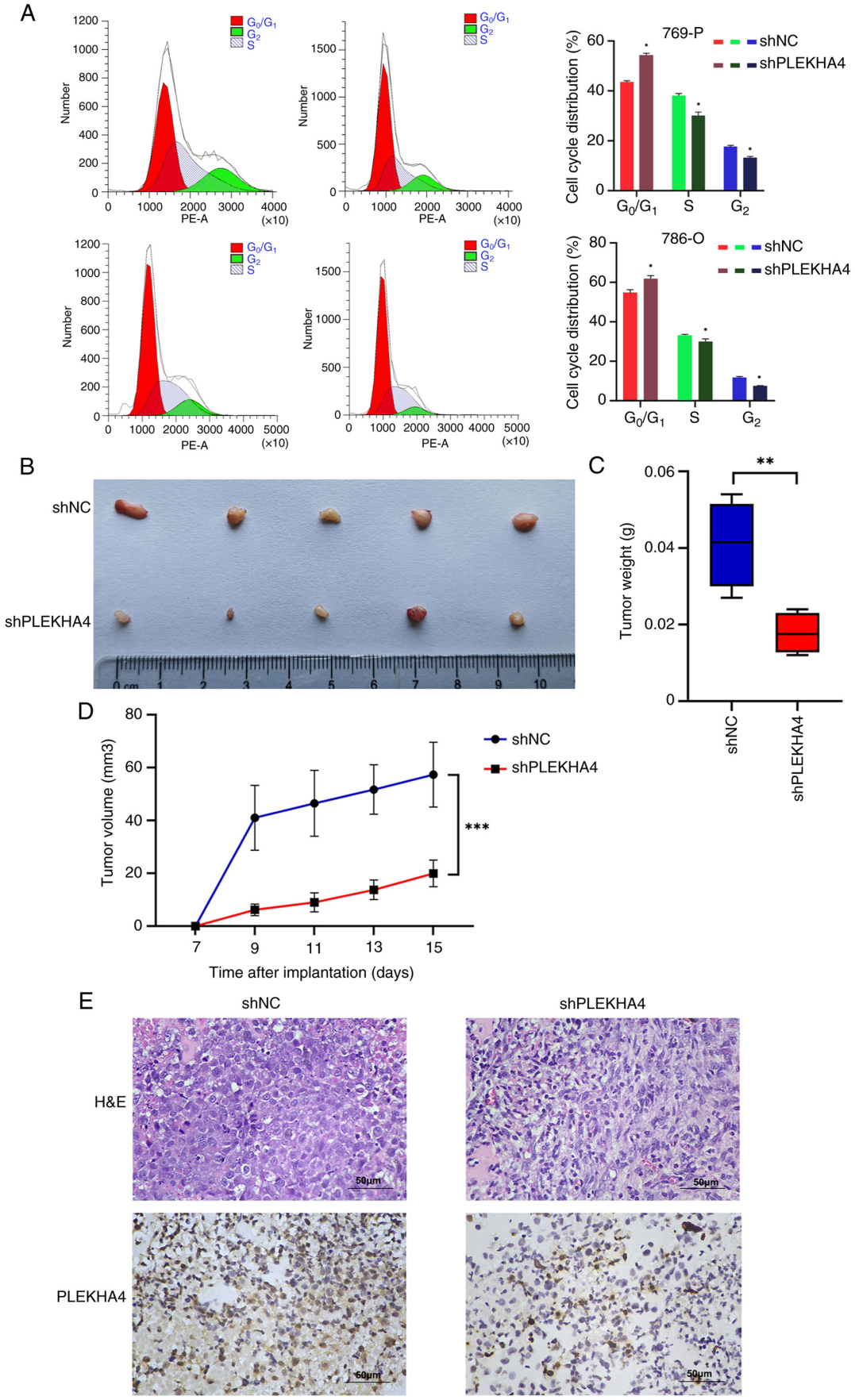

Figure 4. Knockdown of PLEKHA4 suppresses the proliferation of kidney renal clear cell carcinoma cells compared with control cells carcinoma cells *in vivo*. (A) Cell cycle was analyzed in 769-P and 786-O cell lines after PLEKHA4 knockdown. (B) Tumors were collected and images were captured. Tumor (C) weight and (D) volume. (E) Histology of tumors stained with H&E and expression of PLEKHA4 detected by immunohistochemistry. *P<0.05, **P<0.01, ***P<0.001 vs. shNC or as indicated. PLEKHA4, pleckstrin homology domain-containing family A member 4; H&E, hematoxylin and eosin; sh, short hairpin; NC, negative control.

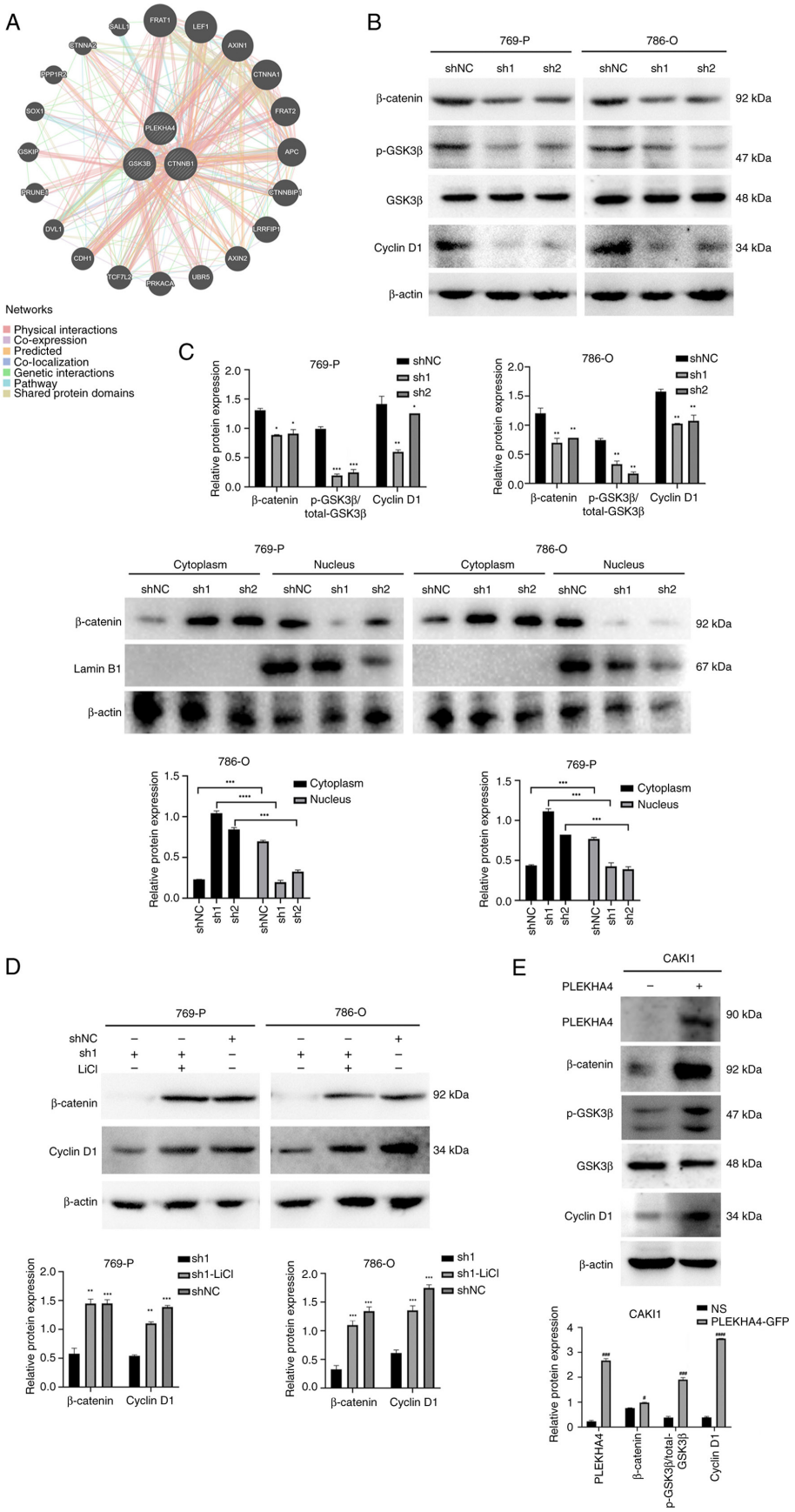

Figure 5. PLEKHA4 knockdown inhibits the Wnt/β-catenin signaling pathway. (A) Functional association networks of PLEKHA4 and β-catenin-related genes. (B) Western blotting showed that knockdown of PLEKHA4 decreased the expression of β-catenin, p-GSK3β and cyclin D1. (C) Effects of PLEKHA4 knockdown on subcellular localization of β-catenin in 769-P and 786-O cells. (D) LiCl reverses the changes induced by PLEKHA4 knockdown in related proteins. (E) PLEKHA4 overexpression increases expression of β-catenin, p-GSK3β and cyclin D1. *P<0.05, **P<0.01, ***P<0.001, ****P<0.0001 vs. shNC or as otherwise indicated. $^{\#}$P<0.05, $^{\#\#\#}$P<0.001, $^{\#\#\#\#}$P<0.0001 vs. NS. PLEKHA4, pleckstrin homology domain-containing family A member 4; sh, short hairpin; NC, negative control; NS, empty vector; p-, phosphorylated.

but did not specifically explore apoptosis. The present results indicated that PLEKHA4 was also upregulated in KIRC and knocking down PLEKHA4 inhibited cell proliferation, which may lead to increased apoptosis. The aforementioned data highlight the role of PLEKHA4 in promoting tumor progression, potentially via modulation of apoptotic pathways and cell proliferation.

Previous studies have highlighted the role of PLEKHA4 in promoting aberrant Wnt signaling in mouse cells (C57MG, C57/MV7) and human melanoma proliferation (6-8). Furthermore, PLEKHA4 has been implicated in modulating chemokines and JAK/STAT pathways, along with impacting the cell cycle in glioma, suggesting its potential use as a prognostic biomarker for glioma (7). Nevertheless, further data is needed to confirm its utility in different grades of KIRC, given the current limitations of bioinformatics analysis, due to the limited availability of clinical tissue RNA sequencing data. Moreover, more clinical data must be collected due to the shortage of clinical tissue samples. Studies have identified Von Hippel-Lindau (VHL) tumor suppressor gene as being closely linked to RCC (17,18), highlighting its association with the pathogenesis of this malignancy. Notably, VHL has been identified as a target of β-catenin, indicating the potential importance of Wnt/β-catenin signaling in RCC development (18). In the present study, the knockdown of PLEKHA4 in KIRC cells notably influenced the expression of classical Wnt/β-catenin targets, such as cyclin D1, leading to cell cycle arrest at the G_1/S phase. This aligns with findings from previous research (19). An aberrant cell cycle is a recognized hallmark of cancer, with cyclin D1 playing a key role in regulating the G_1-S transition (9). Numerous studies have reported elevated cyclin D1 expression in RCC (10,17,19). Cyclin D1 can be transcriptionally activated by β-catenin within the nucleus (18,20).

The canonical Wnt signaling pathway is a highly conserved regulatory mechanism key for embryonic development and the maintenance of adult tissue homeostasis. Perturbations in this pathway can contribute to a spectrum of diseases, including congenital malformations, neurodegenerative disorders, diabetes and diverse forms of cancer (21,22). A key event in the pathway entails the nuclear translocation of β-catenin. Upon binding of Wnt ligands, inhibition of the β-catenin destruction complex in the cytoplasm occurs. This leads to the accumulation of β-catenin, facilitating its translocation into the nucleus (21,22). The translocation of β-catenin into the nucleus results in increased expression of c-Myc and MMPs, thereby promoting the advancement of cancer (23,24). c-Myc serves a vital role in tumorigenesis across various human tissues (25), while MMPs are linked to metastasis and angiogenesis, further driving cancer progression (24). The present study conducted a rescue assay to counteract the effects of PLEKHA4 knockdown. Notably, the Wnt/β-catenin activator LiCl effectively reversed the alterations induced by PLEKHA4 knockdown. Additionally, the overexpression of PLEKHA4 in a KIRC cell line with low PLEKHA4 expression (CAKI1) activated the Wnt/β-catenin signaling pathway. These findings provide crucial supplementary evidence supporting the regulatory role of PLEKHA4 in Wnt/β-catenin signaling in KIRC cells. Targeted inhibition of Wnt signaling may be a promising strategy for the development of novel anticancer therapy if it can be accomplished selectively to minimize adverse effects on healthy tissue (26-28). The present study used 769-P, 786-O and CAKI1 cells, which have been widely used in renal cancer studies, and there is a substantial body of literature reporting their biological characteristics and experimental responses (29-32). By using the 769-P, 786-O and CAKI1 cell lines, more representative and broadly applicable experimental results can be obtained.

In conclusion, PLEKHA4 was upregulated in KIRC and was associated with cell proliferation. Knockdown of PLEKHA4 suppressed β-catenin signaling and impeded its nuclear translocation. However, the specific mechanism by which PLEKHA4 interacts with β-catenin remains unexplored. It is unclear whether PLEKHA4 directly binds to β-catenin or facilitates its translocation through intermediary molecules. Future investigations are warranted to elucidate this potential interaction.

Acknowledgements

Not applicable.

Funding

The present study was supported by the Project of Education Department of the Jilin Province of China (grant no. JJKH20180910KJ).

Availability of data and materials

The data generated in the present study may be requested from the corresponding author.

Authors' contributions

YY, GA and SC performed the experiments. DX made substantial contributions to data analysis. XL and LD made substantial contributions to the bioinformatics analysis, drafted the manuscript, critically reviewed the manuscript for important intellectual content and constructed the figures. LL and TJ made substantial contributions to the conception or design of the work. LL and TJ confirm the authenticity of all the raw data. All authors read and approved the final version of the manuscript.

Ethics approval and consent to participate

The present study was approved by the Laboratory Animal Ethics Committee Yanbian University (approval no. YD20230911020). All methods were performed in accordance with Yanbian University Laboratory Animal Management Rules.

Patient consent for publication

Not applicable.

Competing interests

The authors declare that they have no competing interests.

References

1. Bahadoram S, Davoodi M, Hassanzadeh S, Bahadoram M, Barahman M and Mafakher L: Renal cell carcinoma: An overview of the epidemiology, diagnosis, and treatment. G Ital Nefrol 39: 2022-vol3, 2022.
2. Bex A, Albiges L, Ljungberg B, Bensalah K, Dabestani S, Giles RH, Hofmann F, Hora M, Kuczyk MA, Lam TB, *et al*: Updated European association of urology guidelines for cytoreductive nephrectomy in patients with synchronous metastatic clear-cell renal cell carcinoma. Eur Urol 74: 805-809, 2018.
3. Botrugno OA, Fayard E, Annicotte JS, Haby C, Brennan T, Wendling O, Tanaka T, Kodama T, Thomas W, Auwerx J and Schoonjans K: Synergy between LRH-1 and beta-catenin induces G1 cyclin-mediated cell proliferation. Mol Cell 15: 499-509, 2004.
4. Chow WH, Dong LM and Devesa SS: Epidemiology and risk factors for kidney cancer. Nat Rev Urol 7: 245-257, 2010.
5. Gobbo S, Eble JN, Grignon DJ, Martignoni G, MacLennan GT, Shah RB, Zhang S, Brunelli M and Cheng L: Clear cell papillary renal cell carcinoma: A distinct histopathologic and molecular genetic entity. Am J Surg Pathol 32: 1239-1245, 2008.
6. Sung H, Ferlay J, Siegel RL, Laversanne M, Soerjomataram I, Jemal A and Bray F: Global cancer statistics 2020: GLOBOCAN estimates of incidence and mortality worldwide for 36 cancers in 185 countries. CA Cancer J Clin 71: 209-249, 2021.
7. Gao X, Liu Y, Hong S, Yang H, Guan B and Ma X: PLEKHA4 is associated with tumour microenvironment, stemness, proliferation and poor prognosis of gliomas. J Integr Neurosci 22: 135, 2023.
8. Shami Shah A, Batrouni AG, Kim D, Punyala A, Cao W, Han C, Goldberg ML, Smolka MB and Baskin JM: PLEKHA4/kramer attenuates dishevelled ubiquitination to modulate Wnt and planar cell polarity signaling. Cell Rep 27: 2157-2170.e8, 2019.
9. Tanton H, Sewastianik T, Seo HS, Remillard D, Pierre RS, Bala P, Aitymbayev D, Dennis P, Adler K, Geffken E, *et al*: A novel β-catenin/BCL9 complex inhibitor blocks oncogenic Wnt signaling and disrupts cholesterol homeostasis in colorectal cancer. Sci Adv 8: eabm3108, 2022.
10. Nusse R and Clevers H: Wnt/β-catenin signaling, disease, and emerging therapeutic modalities. Cell 169: 985-999, 2017.
11. Xu Q, Krause M, Samoylenko A and Vainio S: Wnt signaling in renal cell carcinoma. Cancers (Basel) 8: 57, 2016.
12. Xu X, Zhang M, Xu F and Jiang S: Wnt signaling in breast cancer: Biological mechanisms, challenges and opportunities. Mol Cancer 19: 165, 2020.
13. Li Y, Xiao X, Chen H, Chen Z, Hu K and Yin D: Transcription factor NFYA promotes G1/S cell cycle transition and cell proliferation by transactivating cyclin D1 and CDK4 in clear cell renal cell carcinoma. Am J Cancer Res 10: 2446-2463, 2020.
14. Ji J, Xu Y, Xie M, He X, Ren D, Qiu T, Liu W, Chen Z, Shi W, Zhang Z, *et al*: VHL-HIF-2α axis-induced SEMA6A upregulation stabilized β-catenin to drive clear cell renal cell carcinoma progression. Cell Death Dis 14: 83, 2023.
15. Jones J, Out H, Spentzos D, Kolia S, Inan M, Beecken WD, Fellbaum C, Gu X, Joseph M, Pantuck AJ, *et al*: Gene signatures of progression and metastasis in renal cell cancer. Clin Cancer Res 11: 5730-5739, 2005.
16. Wozniak MB, Le Calvez-Kelm F, Abedi-Ardekani B, Byrnes G, Durand G, Carreira C, Michelon J, Janout V, Holcatova I, Foretova L, *et al*: Integrative genome-wide gene expression profiling of clear cell renal cell carcinoma in Czech Republic and in the United States. PLoS One 8: e57886, 2013.
17. MacDonald BT, Tamai K and He X: Wnt/beta-catenin signaling: Components, mechanisms, and diseases. Dev Cell 17: 9-26, 2009.
18. Maretzky T, Reiss K, Ludwig A, Buchholz J, Scholz F, Proksch E, de Strooper B, Hartmann D and Saftig P: ADAM10 mediates E-cadherin shedding and regulates epithelial cell-cell adhesion, migration, and beta-catenin translocation. Proc Natl Acad Sci USA 102: 9182-9187, 2005.
19. Shami Shah A, Cao X, White AC and Baskin JM: PLEKHA4 promotes Wnt/β-catenin signaling-mediated G_1-S transition and proliferation in melanoma. Cancer Res 81: 2029-2043, 2021.
20. Hedberg Y, Davoodi E, Roos G, Ljungberg B and Landberg G: Cyclin-D1 expression in human renal-cell carcinoma. Int J Cancer 84: 268-272, 1999.
21. Albrecht LV, Tejeda-Muñoz N and De Robertis EM: Cell Biology of canonical Wnt signaling. Annu Rev Cell Dev Biol 37: 369-389, 2021.
22. Niehrs C: The complex world of WNT receptor signalling. Nat Rev Mol Cell Biol 13: 767-779, 2012.
23. Bian J, Dannappel M, Wan C and Firestein R: Transcriptional regulation of Wnt/β-catenin pathway in colorectal cancer. Cells 9: 2125, 2020.
24. Hashemi M, Hasani S, Hajimazdarany S, Ghadyani F, Olyaee Y, Khodadadi M, Ziyarani MF, Dehghanpour A, Salehi H, Kakavand A, *et al*: Biological functions and molecular interactions of Wnt/β-catenin in breast cancer: Revisiting signaling networks. Int J Biol Macromol 232: 123377, 2023.
25. Zhang Y and Wang X: Targeting the Wnt/β-catenin signaling pathway in cancer. J Hematol Oncol 13: 165, 2020.
26. Krishnamurthy N and Kurzrock R: Targeting the Wnt/beta-catenin pathway in cancer: Update on effectors and inhibitors. Cancer Treat Rev 62: 50-60, 2018.
27. Neiheisel A, Kaur M, Ma N, Havard P and Shenoy AK: Wnt pathway modulators in cancer therapeutics: An update on completed and ongoing clinical trials. Int J Cancer 150: 727-740, 2022.
28. Zhang N, Wei P, Gong A, Chiu WT, Lee HT, Colman H, Huang H, Xue J, Liu M, Wang Y, *et al*: FoxM1 promotes β-catenin nuclear localization and controls Wnt target-gene expression and glioma tumorigenesis. Cancer Cell 20: 427-442, 2011.
29. Li P, Chen T, Kuang P, Liu F, Li Z, Liu F, Wang Y, Zhang W and Cai X: Aurora-A/FOXO3A/SKP2 axis promotes tumor progression in clear cell renal cell carcinoma and dual-targeting Aurora-A/SKP2 shows synthetic lethality. Cell Death Dis 13: 606, 2022.
30. Swiatek M, Jancewicz I, Kluebsoongnoen J, Zub R, Maassen A, Kubala S, Udomkit A, Siedlecki JA, Sarnowski TJ and Sarnowska E: Various forms of HIF-1α protein characterize the clear cell renal cell carcinoma cell lines. IUBMB Life 72: 1220-1232, 2020.
31. He W, Cong Z, Niu C, Cheng F, Yi T, Yao Z, Zhang Y, Jiang X, Sun X, Niu Z and Fu Q: A prognostic signature based on genes associated with m6A/m5C/m1A/m7G modifications and its immunological characteristics in clear cell renal cell carcinoma. Sci Rep 14: 18708, 2024.
32. Yin X, Wang J and Zhang J: Identification of biomarkers of chromophobe renal cell carcinoma by weighted gene co-expression network analysis. Cancer Cell Int 18: 206, 2018.